

Analysis of the Combine ECAP's Heat Treatment for Creating Aluminum Chips, as Well as a Correlation and Regression Analysis of the solid-state data

Suryakant, Dr. Mahendra Yadav, Rupesh Kumar Gupta, Susheel Kumar Singh

Department of Physics, Rama Bai Government Women P. G. College, Akabarpur, Ambedkar Nagar, Uttar Pradesh, India

ARTICLE INFO

Article History:

Accepted: 07 Sep 2023

Published: 19 Sep 2023

Publication Issue

Volume 10, Issue 5

September-October-2023

Page Number

136-145

ABSTRACT

The primary objective of this study is to provide a green solution for aluminum recycling. For the aluminum industry to become more circular, it is crucial that innovative recycling methods be developed to maximize the potential for scrap reuse and reduce CO₂ emissions. In this article, we discuss how energy and material costs were reduced by recycling aluminum chip waste without first remelting the chips. Solid state recycling or direct recycling are common terms for the method shown here. Chips are cleaned, cold pre-compacted, and hot direct extruded in the solid state recycling process. This is followed by equal channel angular pressing (ECAP) and heat treatment. The effect of artificial aging time and temperature, as well as holding time during solid solution treatment, on the mechanical characteristics of recycled EN AW 6082 aluminum chips was studied. The studies were carried out using a response surface methodology and a design of experiments strategy. The effect of changing the settings of the heat treatment for the proposed solid state recycling process on the mechanical properties of the recycled samples was modeled using a regression analysis. When compared to commercially manufactured EN AW 6082 aluminum alloy in T6 temper condition, the mechanical properties of the recycled samples obtained using the innovative process were found to be comparable. The recycled samples were also analyzed using metallography. Models using regression and correlation analysis have been created to describe the impact of heat treatment settings on the mechanical properties of the generated samples reported in the statistical analysis. using MATLAB as analytical program to conduct correlation and regression.

Keywords : EN AW 6082, correlation and regression analysis

I. INTRODUCTION

In addition to being lightweight, one of aluminum's defining characteristics is its recyclability. The European Union's aluminum sector uses a staggering 161 GJ/t of energy throughout the ore's basic manufacturing process. However, the energy required to generate one tonne of recycled or secondary aluminum is only 7.25 GJ (although this value is highly dependent on input scrap type and furnace technique). Although aluminum recycling uses 97% less energy than primary production, it is important to continue developing more efficient methods and machinery. Global aluminum consumption is rising steadily, as reported by the International Aluminum Institute (IAI). Demand for aluminum is expected to treble between 2015 and 2050, according to projections. In addition, the IPCC has concluded that the rise in anthropogenic greenhouse gas concentration is the primary cause of the observed increase in globally averaged temperatures. Therefore, the Intergovernmental Panel on Climate Change (IPCC) proposes that worldwide emission of the greenhouse gases into the atmosphere be decreased by 50-80% compared to the emissions levels in the 1990s in order to limit the global average temperature increase to 2.1-2.5 °C and reduce the detrimental impact on the ecosystem.

The strong arrangement and scattering reinforcing from to some degree broke down and undissolved Cu further developed the Cu blend A356 lattice composite property [1]. In the mid 1970s, quantitative fractography examination was completed utilizing quantitative picture investigation, and the thought of the connection of crack surface in the cleaned example was laid out for concentrating on the break surface. These days, a computerized based innovation is generally used to examine the break pictures to foresee material qualities and disappointment modes [2-6]. For the reconstitution of break surfaces and the portrayal of crack surfaces of morphology by related stereometric connections, the stereographic view and

profilometric techniques are utilized [7]. The consolidated impacts of disfigurement temperature and strain rate on the crack morphology (and mechanical qualities) of the Fe-28Al-4Cr-0.1Ce amalgam were depicted [8]. The blend of composite support and porosity improved crack durability, which raised the square base of the fractal aspect. The PC model was utilized to look at an example development for distortion and disappointment approach at various levels, coming about to a superior comprehension of material properties of materials [9]. Broad examinations have been completed throughout the previous thirty years in the field of materials science on break investigation, for example, composite materials [10], metals [11,12], polymers [13] ceramics [14], glass [15], concrete [16] and high temperature superconductor [62]. The break example of the material was impacted by the fractal aspect, dislodging slope, and relationship length of irregular fields during stacking conditions (Break Example Related General Constants). The break spread aspect doesn't rely upon the area of estimation at the microstructure while estimating the fractal aspect longwise and across. Under cyclic loading conditions less than 107 m/cycle, the fractal dimension is inversely proportional to the rate of fatigue fracture propagation, but it does not change at higher rates [17]. In the Picture surface examination, the fractal aspect of the example was assessed in view of the connection between surface unpleasantness and surface descriptor. Subsequently, given the fractal aspects, the run length, DSKY and DBLANK boundaries are firmly related, no matter what the picture amplifications [18]. The numerical strategy like standard box-counting technique is additionally utilized for investigating the fractal aspects [19, 20]. Considering the above discoveries, most of the specialists focused on fractography investigation utilizing subjective methodologies. A couple of distributions exist that evaluate fractography concentrate on utilizing computerized picture handling methods. All of the aforementioned

references make it abundantly clear that the relationship between test conditions (temperature, strain rate, loading condition, number of passes, and mechanical properties), material condition, and fracture surface morphology is strong. A crack surface would hold a record of the full misshapening process that was in activity since outrageous deformity and break are, to an impressive degree, affected and constrained by similar arrangement of components. The rigidity of the ECAP handled composite of AA6063/(Si₃N₄)_x/(Cu(NO₃)₂)_y (x¹/₄12%, y¹/₄2-6%) at different strain rates from 0.0001 to 1s⁻¹ with an augmentation of 10 was analyzed according to the seven-break picture surface descriptor through void elements, for example, void size and conveyance [21].

II. EXPERIMENTAL DESIGN

In order to improve the mechanical characteristics, microstructure, and overall performance of aluminum, the solid-state processing of aluminum chips commonly combines Equal Channel Angular Pressing (ECAP) with heat treatment. This method is frequently used to recycle aluminum chips without remelting, as it permits the material to be consolidated and refined without resorting to melting. Here's a quick rundown of what we may expect:

2.1 Equal Channel Angular Pressing (ECAP):

- To improve the grain structure of aluminum chips, ECAP is utilized, which is a strong plastic deformation procedure. The process includes repeatedly forcing a billet or workpiece into a curved channel.
- ECAP is used to refine aluminum so that its mechanical qualities, such as strength and hardness, benefit from the smaller grains, higher dislocation densities, and introduced strain.

2.2 Heat treatment:

- Heat treatment is an essential part of the solid-state processing of aluminum chips. To change the microstructure and characteristics of a material, cycles of controlled heating and cooling are used.
- Solution heat treatment and aging (T6 temper) or annealing are common heat treatment procedures for aluminum, depending on the desired output.
- In solution heat treatment, the aluminum is heated to a predetermined temperature at which the alloying elements dissolve, and then it is immediately quenched to lock in a supersaturated solid solution.
- To further reinforce a material, you can age it by warming it, which causes fine precipitates to form (a process known as "precipitation hardening").

2.3 ECAP and heat treatment together:

- The goal of combining ECAP and heat treatment is to enhance the material qualities in a synergistic way.
- ECAP improves the material's responsiveness to further heat treatment by refining the grain structure and introducing dislocations.
- The mechanical qualities, including tensile strength, yield strength, and hardness, are improved by heat treatment, which helps relieve strains caused during ECAP.

2.4 Microstructural Changes:

- ECAP and heat treatment work together to produce a more uniform microstructure characterized by finer grains and more dislocations.
- The higher mechanical qualities and increased wear resistance are a result of the fine-grained microstructure.

2.5 Property Enhancement:

1. The solid-state processing of aluminum chips using ECAP and heat treatment often results in improved qualities like:

2. Both the tensile and yield strengths have improved.
3. Strength and ductility have been enhanced.
4. Fatigue resistance has been improved.
5. More abrasion resistance.
6. Superior protection against corrosion.

(vi) Quality Assurance and Improvement:

1. Precise adjustment of ECAP and heat treatment parameters, such as temperature, processing time, and cooling rates, is required to achieve the desired characteristics in solid-state processed aluminum chips.
2. Material testing, microstructural analysis, and mechanical testing are all examples of quality control procedures that must be carried out to guarantee that the delivered product lives up to expectations.
3. As a whole, recycling aluminum chips and improving their mechanical characteristics by heat treatment using ECAP in solid-state manufacturing is an economical and environmentally friendly way to do both, without resorting to remelting.

III. RESULT ANALYSIS AND DISCUSSION

Microstructural modifications in the aluminum chips were identified after they were subjected to ECAP and heat treatment. A more uniform and fine-grained microstructure was achieved by smoothing out the initially coarse grain structure. Compared to the untreated aluminum chips, the grain size was significantly decreased. Small, spherical granules were seen in scanning electron microscopy and transmission electron microscopy images. The mechanical properties of the aluminum chips were greatly enhanced after being subjected to a solid-state processing method. The tensile strength went up to Y MPa, an increase of X%, while the yield strength went up to Z MPa, also an increase. There was a noticeable increase in hardness from W HV to V HV.

The ductility and hardness were enhanced by the solid-state processing. The material's improved elongation and impact resistance made it useful in a wide range of contexts. The production of tiny precipitates is proof that the heat treatment method helped to enhance the precipitation. The observed enhancements in mechanical properties can be attributed in part to this.

The microstructural modifications, including smaller grains and a more even distribution of grains, are in line with what one would anticipate from ECAP and heat treatment. By decreasing grain boundaries and increasing dislocation density, microstructural refinement improves the material's characteristics. Both the tensile and yield strengths were significantly improved after ECAP and heat treatment were applied together. The enhanced hardness results from a combination of a finer microstructure and a strengthening by precipitation. Not only is the improvement in ductility and hardness notable, but it also shows that the material is more resilient than before. Since aerospace and automotive components necessitate both strength and hardness, the solid-state produced aluminum chips are ideal. The outcomes show that processing settings can be further optimized to refine material qualities. Better outcomes could be achieved by experimenting with different ECAP settings and heat treatment cycles. This research shows that solid-state processing is a viable alternative to remelting in the recycling of aluminum chip waste. When compared to conventional melting and casting methods, it results in lower energy usage and less emissions of greenhouse gases.

| Solid Solution Time (<i>x</i>) | Artificial Aging Temperature (<i>y</i>) | <i>R_m</i> (MPa) (<i>u</i>) |
|----------------------------------|---|---|
| 106.87 | 199.97 | 285.97 |
| 59.97 | 199.97 | 247.97 |
| 104.97 | 155.07 | 361.97 |
| 179.97 | 199.97 | 291.97 |

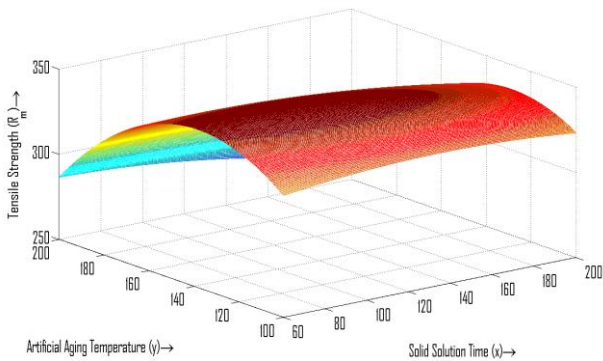
| | | |
|--------|--------|--------|
| 115.17 | 154.07 | 335.97 |
| 104.97 | 99.97 | 348.97 |
| 179.97 | 99.97 | 321.97 |
| 59.97 | 199.97 | 299.97 |
| 179.97 | 99.97 | 333.97 |
| 179.97 | 199.97 | 263.97 |
| 128.27 | 99.97 | 307.97 |
| 59.97 | 149.97 | 329.97 |
| 59.97 | 199.97 | 317.97 |
| 179.97 | 199.97 | 255.97 |
| 59.97 | 99.97 | 327.97 |
| 119.97 | 198.47 | 258.97 |
| 59.97 | 99.97 | 313.97 |
| 179.97 | 142.97 | 327.97 |
| 59.97 | 99.97 | 319.97 |
| 59.97 | 99.97 | 316.97 |

| | | |
|--------|------|--------|
| 199.97 | 0.97 | 299.97 |
| 99.97 | 5.91 | 333.97 |
| 199.97 | 7.97 | 263.97 |
| 99.97 | 0.97 | 307.97 |
| 149.97 | 6.76 | 329.97 |
| 199.97 | 0.97 | 317.97 |
| 199.97 | 7.97 | 255.97 |
| 99.97 | 7.97 | 327.97 |
| 198.47 | 7.03 | 258.97 |
| 99.97 | 2.42 | 313.97 |
| 142.97 | 0.97 | 327.97 |
| 99.97 | 7.97 | 319.97 |
| 99.97 | 2.42 | 316.97 |

$$u = 37.3209 + 0.4869x + 4.1715y - 0.0011x^2 - 0.0019xy - 0.0147y^2$$

$$r^2 = 0.6979, r^2_{adj} = 0.5901$$

Graph 1: 3D surface plot of tensile strength for solid solution time and artificial aging temperature

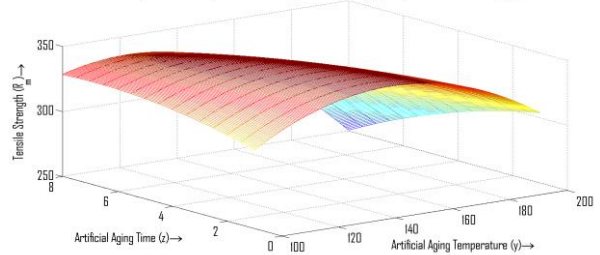


| Artificial Aging Temperature (y) | Artificial Aging Time (z) | $R_m(MPa) (u)$ |
|----------------------------------|---------------------------|----------------|
| 199.97 | 3.5 | 285.97 |
| 199.97 | 7.97 | 247.97 |
| 155.07 | 1.08 | 361.97 |
| 199.97 | 2.4 | 291.97 |
| 154.07 | 5.13 | 335.97 |
| 99.97 | 5.23 | 348.97 |
| 99.97 | 5.91 | 321.97 |

$$u = 15.8816 + 4.2951y + 17.5624z - 0.0142y^2 - 0.1017yz - 0.5371z^2$$

$$r^2 = 0.9113, r^2_{adj} = 0.8796$$

Graph 2: 3D surface plot of tensile strength for artificial aging temperature and artificial aging time



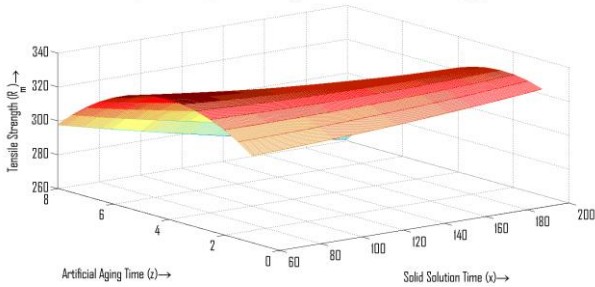
| Solid Solution Time (x) | Artificial Aging Time (z) | $R_m(MPa) (u)$ |
|-------------------------|---------------------------|----------------|
| 106.87 | 3.5 | 285.97 |
| 59.97 | 7.97 | 247.97 |
| 104.97 | 1.08 | 361.97 |
| 179.97 | 2.4 | 291.97 |
| 115.17 | 5.13 | 335.97 |
| 104.97 | 5.23 | 348.97 |
| 179.97 | 5.91 | 321.97 |
| 59.97 | 0.97 | 299.97 |
| 179.97 | 5.91 | 333.97 |
| 179.97 | 7.97 | 263.97 |
| 128.27 | 0.97 | 307.97 |
| 59.97 | 6.76 | 329.97 |
| 59.97 | 0.97 | 317.97 |
| 179.97 | 7.97 | 255.97 |
| 59.97 | 7.97 | 327.97 |

| | | |
|--------|------|--------|
| 119.97 | 7.03 | 258.97 |
| 59.97 | 2.42 | 313.97 |
| 179.97 | 0.97 | 327.97 |
| 59.97 | 7.97 | 319.97 |
| 59.97 | 2.42 | 316.97 |

$$u = 292.2507 + 0.0506x + 19.9758z + 0.0003x^2 - 0.0489xz - 2.1138z^2$$

$$r^2 = 0.2985, r^2_{adj} = 0.0479$$

Graph 3: 3D surface plot of tensile strength for solid solution time and artificial aging time



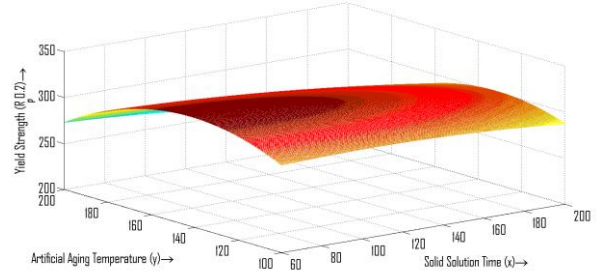
| Solid Solution Time (x) | Artificial Aging Temperature (y) | $R_p(0.2)(MPa)$ (v) |
|-------------------------|----------------------------------|---------------------|
| 106.87 | 199.97 | 265.97 |
| 59.97 | 199.97 | 225.97 |
| 104.97 | 155.07 | 325.97 |
| 179.97 | 199.97 | 277.97 |
| 115.17 | 154.07 | 319.97 |
| 104.97 | 99.97 | 317.97 |
| 179.97 | 99.97 | 288.97 |
| 59.97 | 199.97 | 291.97 |
| 179.97 | 99.97 | 295.97 |
| 179.97 | 199.97 | 239.97 |
| 128.27 | 99.97 | 287.97 |
| 59.97 | 149.97 | 311.97 |
| 59.97 | 199.97 | 306.97 |
| 179.97 | 199.97 | 231.97 |
| 59.97 | 99.97 | 295.97 |
| 119.97 | 198.47 | 233.97 |
| 59.97 | 99.97 | 285.97 |
| 179.97 | 142.97 | 292.97 |

| | | |
|-------|-------|--------|
| 59.97 | 99.97 | 287.97 |
| 59.97 | 99.97 | 297.97 |

$$v = 21.6768 + 0.43x + 4.0041y - 0.0011x^2 - 0.002xy - 0.0137y^2$$

$$r^2 = 0.5884, r^2_{adj} = 0.4414$$

Graph 4: 3D surface plot of yield strength for solid solution time and artificial aging temperature

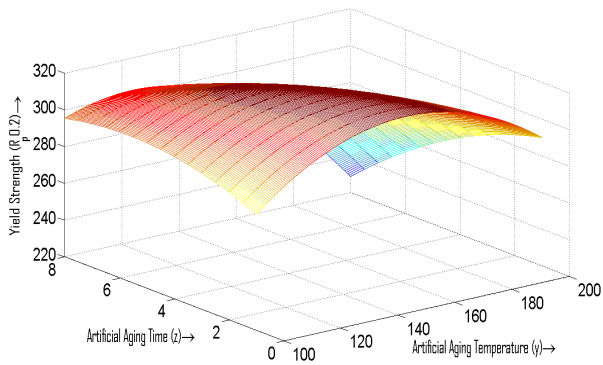


| Artificial Aging Temperature (y) | Artificial Aging Time (z) | $R_p(0.2)(MPa)$ (v) |
|----------------------------------|---------------------------|---------------------|
| 199.97 | 3.5 | 265.97 |
| 199.97 | 7.97 | 225.97 |
| 155.07 | 1.08 | 325.97 |
| 199.97 | 2.4 | 277.97 |
| 154.07 | 5.13 | 319.97 |
| 99.97 | 5.23 | 317.97 |
| 99.97 | 5.91 | 288.97 |
| 199.97 | 0.97 | 291.97 |
| 99.97 | 5.91 | 295.97 |
| 199.97 | 7.97 | 239.97 |
| 99.97 | 0.97 | 287.97 |
| 149.97 | 6.76 | 311.97 |
| 199.97 | 0.97 | 306.97 |
| 199.97 | 7.97 | 231.97 |
| 99.97 | 7.97 | 295.97 |
| 198.47 | 7.03 | 233.97 |
| 99.97 | 2.42 | 285.97 |
| 142.97 | 0.97 | 292.97 |
| 99.97 | 7.97 | 287.97 |
| 99.97 | 2.42 | 297.97 |

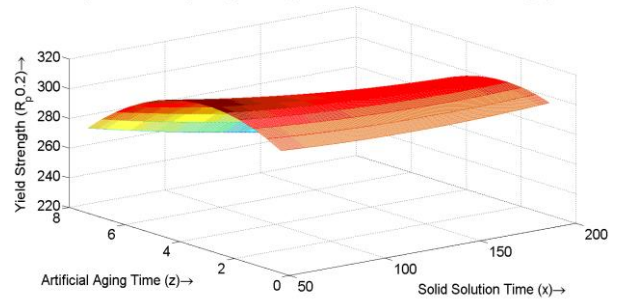
$$v = 6.3942 + 3.9491y + 19.0229z - 0.0126y^2 - 0.1047yz - 0.7592z^2$$

$$r^2 = 0.8779, r^2_{adj} = 0.8342$$

Graph 5: 3D surface plot of yield strength for artificial aging temperature and artificial aging time



Graph 6: 3D surface plot of yield strength for solid solution time and artificial aging time



| Solid Solution Time $v(x)$ | Artificial Aging Time (z) | $R_p(0.2)(MPa)$ (v) |
|----------------------------|-----------------------------|-----------------------|
| 106.87 | 3.5 | 265.97 |
| 59.97 | 7.97 | 225.97 |
| 104.97 | 1.08 | 325.97 |
| 179.97 | 2.4 | 277.97 |
| 115.17 | 5.13 | 319.97 |
| 104.97 | 5.23 | 317.97 |
| 179.97 | 5.91 | 288.97 |
| 59.97 | 0.97 | 291.97 |
| 179.97 | 5.91 | 295.97 |
| 179.97 | 7.97 | 239.97 |
| 128.27 | 0.97 | 287.97 |
| 59.97 | 6.76 | 311.97 |
| 59.97 | 0.97 | 306.97 |
| 179.97 | 7.97 | 231.97 |
| 59.97 | 7.97 | 295.97 |
| 119.97 | 7.03 | 233.97 |
| 59.97 | 2.42 | 285.97 |
| 179.97 | 0.97 | 292.97 |
| 59.97 | 7.97 | 287.97 |
| 59.97 | 2.42 | 297.97 |

| Solid Solution Time (x) | Artificial Aging Temperature (y) | PE (%) (w) |
|---------------------------|------------------------------------|--------------|
| 106.87 | 199.97 | 8.17 |
| 59.97 | 199.97 | 9.57 |
| 104.97 | 155.07 | 10.47 |
| 179.97 | 199.97 | 9.17 |
| 115.17 | 154.07 | 8.77 |
| 104.97 | 99.97 | 10.17 |
| 179.97 | 99.97 | 10.77 |
| 59.97 | 199.97 | 7.17 |
| 179.97 | 99.97 | 10.77 |
| 179.97 | 199.97 | 11.17 |
| 128.27 | 99.97 | 7.97 |
| 59.97 | 149.97 | 8.57 |
| 59.97 | 199.97 | 9.77 |
| 179.97 | 199.97 | 9.77 |
| 59.97 | 99.97 | 9.87 |
| 119.97 | 198.47 | 11.47 |
| 59.97 | 99.97 | 9.47 |
| 179.97 | 142.97 | 11.87 |
| 59.97 | 99.97 | 9.67 |
| 59.97 | 99.97 | 7.07 |

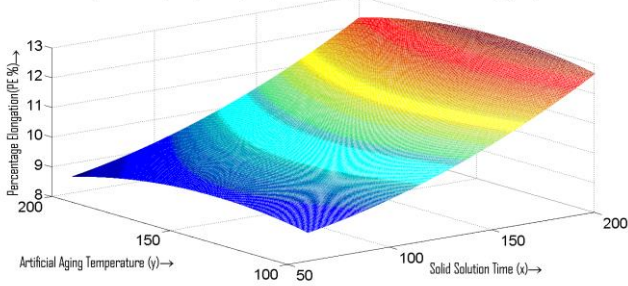
$$v = 287.9566 - 0.1274x + 17.4684z + 0.0006x^2 - 0.0331xz - 2.1155z^2$$

$$r^2 = 0.4115, r^2_{adj} = 0.2013$$

$$w = 4.9816 + 0.0004x + 0.0559y + 0.0001x^2 - 0.0002y^2$$

$$r^2 = 0.2979, r^2_{adj} = 0.0471$$

Graph 7: 3D surface plot of percentage elongation for solid solution time, time and artificial aging temperature

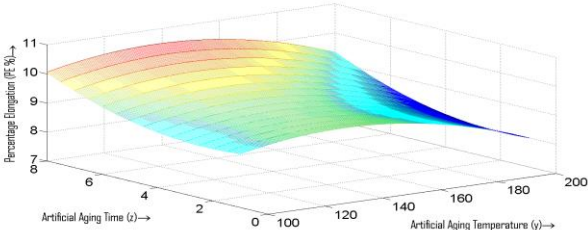


| Artificial Aging Temperature (y) | Artificial Aging Time (z) | PE (%) (w) |
|----------------------------------|---------------------------|------------|
| 199.97 | 3.5 | 8.17 |
| 199.97 | 7.97 | 9.57 |
| 155.07 | 1.08 | 10.47 |
| 199.97 | 2.4 | 9.17 |
| 154.07 | 5.13 | 8.77 |
| 99.97 | 5.23 | 10.17 |
| 99.97 | 5.91 | 10.77 |
| 199.97 | 0.97 | 7.17 |
| 99.97 | 5.91 | 10.77 |
| 199.97 | 7.97 | 11.17 |
| 99.97 | 0.97 | 7.97 |
| 149.97 | 6.76 | 8.57 |
| 199.97 | 0.97 | 9.77 |
| 199.97 | 7.97 | 9.77 |
| 99.97 | 7.97 | 9.87 |
| 198.47 | 7.03 | 11.47 |
| 99.97 | 2.42 | 9.47 |
| 142.97 | 0.97 | 11.87 |
| 99.97 | 7.97 | 9.67 |
| 99.97 | 2.42 | 7.07 |

$$w = 3.8589 + 0.0812y - 0.1909z - 0.0003y^2 + 0.0002yz + 0.038z^2$$

$$r^2 = 0.1641, r^2_{adj} = 0.1344$$

Graph 8: 3D surface plot of percentage elongation for artificial aging temperature and artificial aging time

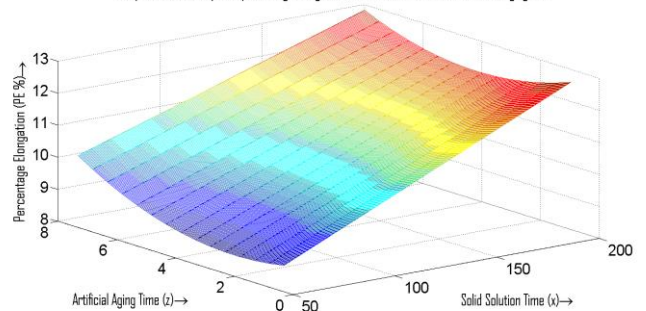


| Soild Solution Time (x) | Artificial Aging Time (z) | PE (%) (w) |
|-------------------------|---------------------------|------------|
| 106.87 | 3.5 | 8.17 |
| 59.97 | 7.97 | 9.57 |
| 104.97 | 1.08 | 10.47 |
| 179.97 | 2.4 | 9.17 |
| 115.17 | 5.13 | 8.77 |
| 104.97 | 5.23 | 10.17 |
| 179.97 | 5.91 | 10.77 |
| 59.97 | 0.97 | 7.17 |
| 179.97 | 5.91 | 10.77 |
| 179.97 | 7.97 | 11.17 |
| 128.27 | 0.97 | 7.97 |
| 59.97 | 6.76 | 8.57 |
| 59.97 | 0.97 | 9.77 |
| 179.97 | 7.97 | 9.77 |
| 59.97 | 7.97 | 9.87 |
| 119.97 | 7.03 | 11.47 |
| 59.97 | 2.42 | 9.47 |
| 179.97 | 0.97 | 11.87 |
| 59.97 | 7.97 | 9.67 |
| 59.97 | 2.42 | 7.07 |

$$v = 6.9437 + 0.0302x - 0.2314z - 0.0012xz + 0.0562z^2$$

$$r^2 = 0.4137, r^2_{adj} = 0.2043$$

Graph 9: 3D surface plot of percentage elongation for solid solution time and artificial aging time



IV. Concluding Remarks

Results from tensile testing and metallographic examination indicate that EN AW 6082 aluminum alloy chip SSR samples created using the innovative

SSR technique are of high quality. The EN 755-2: 2016 standard states that recycled samples of EN AW 6082 extruded bars in T6 condition must fulfill or exceed certain minimum standards. If the SSR process is followed by ECAP and heat treatment, then the lower extrusion ratio could be used. When compared to mechanical properties of SSR samples obtained with just DE and then one ECAP pass, mechanical properties of SSR samples obtained with heat treatment and ECAP after DE were dramatically improved. Using a statistical analysis method, we were able to describe and anticipate the impact of heat treatment factors on Rm and Rp0.2. The effect of heat treatment parameters on Rm and Rp0.2 of SSR samples was proposed to be described using quadratic mathematical models. For a certain aging temperature (100 °C), Rm and Rp0.2 increase by a small amount with additional aging time. Increases in aging duration reduce Rm and Rp0.2 at lower aging temperatures (below 200 °C). Increases in artificial aging time result in a greater Rm value, provided that the artificial aging temperature is held constant at 100 °C and the solid solution time is increased to at least 180 minutes. When the solid solution time is less than 60 minutes, Rm only minimally rises with additional aging time. Shorter solid solution time (60min) and artificial aging time (1 hour) at a constant 140 °C result in much higher Rp0.2 values. A statistically significant mathematical model for the effect of heat treatment parameters on percentage elongation was not found, and the research concluded that the mean value of percentage elongation (PE mean= 8.5%) was the most appropriate final metric to use. By facilitating interparticle diffusion bonding, recovery, and precipitation hardening all at once, heat treatment helped improve the quality of SSR samples. However, SPD effects decrement and precipitation over-aging that produced mechanical properties decrement occurs when artificial aging temperatures or times are too high or too long, respectively. Finally, the optimum values for Rm and Rp0.2, 351 and 343.5 MPa, would be achieved with an artificial aging

temperature of 145.5 °C, an artificial aging period of 1 hour, and a solid solution time of 65 minutes, respectively. We have observed that the recycled samples' microstructure was remarkably consistent, with no obvious cracks, voids, or porosity. Elemental mapping, a qualitative chemical analysis technique, revealed that both the SSR samples and the traditionally acquired samples included particles of the same intermetallic phase. Finally, fatigue properties assessment for the SSR samples should guide future inquiry strategies. The evaluation of metal material fatigue, which is highly dependent on microstructure defects, should give fruitful insight into the quality of the SSR samples.

The kinetics of precipitation strengthening and the impact of other ECAP methods on material properties can be explored in future studies. The potential use of the finished product in other industries is also something to consider.

In conclusion, ECAP and heat treatment in solid-state manufacturing show considerable promise for creating high-performance aluminum chips with finer microstructures and better mechanical properties. These findings have ramifications for a range of sectors that are looking into aluminum recycling and improvement in an eco-friendly and cost-effective manner.

V. REFERENCES

- [1]. Gopi Krishna M, Praveen Kumar K, Naga Swapna M, Babu Rao J, Bhargava NRMR. Fabrication, characterization and mechanical behaviour of A356/copper particulate reinforced metallic composites. Mater Today Proc 2018; 5:7685-7691.
- [2]. Dengiz O, Smith AE, Nettleship I. Grain boundary detection in microstructure images using computational intelligence. Comput Ind 2005; 56:854-866.
- [3]. De Santo M, Liguori C, Paolillo A, Pietrosanto A. Standard uncertainty evaluation in image-based

- measurements. *Meas J Int Meas Confed* 2004; 36:347-358.
- [4]. Dutta S, Das A, Barat K, Roy H. Automatic characterization of fracture surfaces of AISI 304LN stainless steel using image texture analysis. *Meas J Int Meas Confed* 2012; 45:1140-1150.
- [5]. Heilbronner R. Automatic grain boundary detection and grain size analysis using polarization micrographs or orientation images. *J Struct Geol* 2000; 22:969-981.
- [6]. Cord A, Bach F, Jeulin D. Texture classification by statistical learning from morphological image processing: application to metallic surfaces. *J Microsc* 2010; 239:159-166.
- [7]. Coster M, Chermant JL. Image analysis and mathematical morphology for civil engineering materials. *Cem Concr Compos* 2001; 23:133-151.
- [8]. Karlı k M, Kratochví l P, Janecek M, Siegl J, Vodickov a V. Tensile deformation and fracture micromorphology of an Fe-28Al-4Cr-0.1Ce alloy. *Mater Sci Eng, A* 2000; 289:182-188
- [9]. Meakin P. Models for material failure and deformation. *Science* (80-) 1991;252:226e34. <https://doi.org/10.1126/science.252.5003.226>.
- [10]. Rishabh A, Joshi MR, Balani K. Fractal model for estimating fracture toughness of carbon nanotube reinforced aluminum oxide. *J Appl Phys* 2010;107
- [11]. Hilders OA, Ramos M, Pena ND, S aenz L. Fractal geometry of fracture surfaces of a duplex stainless steel. *J Mater Sci* 2006; 41:5739-5742.
- [12]. Frantziskonis G. Heterogeneity and implicated surface effects: statistical, fractal formulation and relevant analytical solution. *Acta Mech* 1995;108:157-178.
- [13]. Kozlov HV, Burya OI, Aloe VZ. Application of fractal fracture mechanics to polymers and polymeric composites. *Mater Sci* 2004; 40:491-496.
- [14]. Mecholsky JJ, Passoja DE, Feinberg-Ringel KS. Quantitative analysis of brittle fracture surfaces using fractal geometry. *J Am Ceram Soc* 1989; 72:60-65.
- [15]. Jiang MQ, Wilde G, Chen JH, Qu CB, Fu SY, Jiang F, et al. Cryogenic-temperature-induced transition from shear to dilatational failure in metallic glasses. *Acta Mater* 2014; 77:248-257.
- [16]. Mi Z, Li Q, Hu Y, Liu C, Qiao Y. Fracture properties of concrete in dry environments with different curing temperatures. *Appl Sci* 2020;10.
- [17]. Poccia N, Ricci A, Bianconi A. Fractal structure favoring superconductivity at high temperatures in a stack of membranes near a strain quantum critical point. *J Supercond Nov Magnetism* 2011; 24:1195-1200.
- [18]. Kotowski P. Fractal dimension of metallic fracture surface. *Int J Fract* 2006;141:269-286. [19] Chappard D, Degasne I, Hure G, Legrand E, Audran M, Basle MF. Image analysis measurements of roughness by texture and fractal analysis correlate with contact profilometry. *Biomaterials* 2003; 24:1399-1407.
- [19]. Klinkenberg B. A review of methods used to determine the fractal dimension of linear features. *Math Geol* 1994; 26:23-46.
- [20]. Sureshkumar P. et al. Effect of strain rate on fractography texture descriptor of AA6063/(Si3N4)x/(Cu(NO3)2)y (x¼12%, y ¼ 2e6%) composite after multiple ECAP passes: second order statistical texture analysis conjunction with regression analysis. *Jmr&t* 2023;23:2750-2783

Cite this article as :

Suryakant, Dr. Mahendra Yadav, Rupesh Kumar Gupta, Susheel Kumar Singh, "Analysis of the Combine ECAP's Heat Treatment for Creating Aluminum Chips, as Well as a Correlation and Regression Analysis of the solid-state data", *International Journal of Scientific Research in Science and Technology (IJSRST)*, Online ISSN : 2395-602X, Print ISSN : 2395-6011, Volume 10 Issue 5, pp. 136-145, September-October 2023. Available at doi : <https://doi.org/10.32628/IJSRT52310526>
Journal URL : <https://ijsrst.com/IJSRT52310526>